

# Dipolar Order Mediated $^1\text{H}\rightarrow^{13}\text{C}$ Cross-Polarization for Dissolution-Dynamic Nuclear Polarization

Stuart J. Elliott<sup>1</sup>, Samuel F. Cousin<sup>1</sup>, Quentin Chappuis<sup>1</sup>, Olivier Cala<sup>1</sup>, Morgan Ceillier<sup>1</sup>, Aurélien Bornet<sup>2</sup>, Sami Jannin<sup>1</sup>

<sup>1</sup>Centre de Résonance Magnétique Nucléaire à Très Hauts Champs - FRE 2034 Université de Lyon / CNRS / Université Claude Bernard Lyon 1 / ENS de Lyon, 5 Rue de la Doua, 69100 Villeurbanne, France

<sup>2</sup>Institut des Sciences et Ingénierie Chimiques, Ecole Polytechnique Fédérale de Lausanne (EPFL), Batochime, CH-1015 Lausanne, Switzerland

Correspondence to: Stuart J. Elliott (stuart-james.elliott@univ-lyon1.fr)

**Abstract.** Magnetic resonance imaging and spectroscopy often suffer from a low intrinsic sensitivity, which can in some cases be circumvented by the use of hyperpolarization techniques. Dissolution-dynamic nuclear polarization offers a way of hyperpolarizing  $^{13}\text{C}$  spins in small molecules, enhancing their sensitivity by up to four orders of magnitude. This is usually performed by direct  $^{13}\text{C}$  polarization, which is straightforward but often takes more than an hour. Alternatively, indirect  $^1\text{H}$  polarization followed by  $^1\text{H}\rightarrow^{13}\text{C}$  polarization transfer can be implemented, which is more efficient and faster but is technically very challenging and hardly implemented in practice. Here we propose to remove the main roadblocks of the  $^1\text{H}\rightarrow^{13}\text{C}$  polarization transfer process by using alternative schemes with: (i) less *rf*-power; (ii) less overall *rf*-energy; (iii) simple *rf*-pulse shapes; and (iv) no synchronized  $^1\text{H}$  and  $^{13}\text{C}$  *rf*-irradiation. An experimental demonstration of such a simple  $^1\text{H}\rightarrow^{13}\text{C}$  polarization transfer technique is presented for the case of  $[1\text{-}^{13}\text{C}]\text{sodium acetate}$ , and is compared with the most sophisticated cross-polarization schemes. A polarization transfer efficiency of  $\sim 0.43$  with respect to cross-polarization was realized, which resulted in a  $^{13}\text{C}$  polarization of  $\sim 8.7\%$  after  $\sim 10$  minutes of microwave irradiation and a single polarization transfer step.

## 1 Introduction

Traditional magnetic resonance imaging (MRI) and spectroscopy (MRS) experiments usually suffer from low sensitivity. Hyperpolarization techniques including dissolution-dynamic nuclear polarization (*d*DNP) can be used to highly polarize a large variety of chemical systems and therefore enhance nuclear magnetic resonance (NMR) signals by several orders of magnitude (Ardenkjær-Larsen et al., 2003). Various applications of *d*DNP have been demonstrated including the study of enzyme kinetics, cell extracts and heteronuclear metabolomics (Bornet et al., 2014; Dumez et al., 2015; Bornet et al., 2016). Most *d*DNP applications involve the use of weakly magnetic isotopes such as  $^{13}\text{C}$ , but excessively long DNP timescales  $\tau_{\text{DNP}}(^{13}\text{C})$  hinder efficient polarization build-up and lead to extended experimental times. Intrinsically sensitive proton nuclear spins do not suffer from such issues and can be polarized quickly and to a greater extent at low temperatures (Hartmann et al., 1973).

The use and optimization of cross-polarization (CP) under *d*DNP conditions (typically at temperatures of about 1.2-1.6 K in superfluid helium) provides a way to substantially boost  $^{13}\text{C}$  polarizations and enhance build-up rates  $1/\tau_{\text{DNP}}(^{13}\text{C})$  (by a factor of up to 40) (Hartmann and Hahn, 1962; Pines et al., 1972; Perez Linde, 2009; Jannin et al., 2011; Bornet et al., 2012; Batel et al., 2012; Bornet et al., 2013; Vuichoud et al., 2016; Cavallès et al., 2018). The technique requires intense  $B_1$ -matching (typically  $> 15$  kHz) of simultaneous  $^1\text{H}$  and  $^{13}\text{C}$  spin-locking radiofrequency (*rf*) fields throughout an optimized contact period (typically  $> 1$  ms). This CP-DNP approach recently turned out to be key for the preparation of transportable hyperpolarization (Ji et al., 2017) where samples are polarized in a CP equipped polarizer and then transported over extended periods (typically hours or days) to the point of use.

This CP approach has been demonstrated on typical *d*DNP samples back in 2012 (Bornet et al., 2012), however, the technique remains challenging today because of its methodological and technical complexity. Indeed, CP under *d*DNP conditions employs

sophisticated pulse sequences, and involves high power and energy *rf*-pulses. Another drawback of CP-DNP is that it can hardly be scaled-up to volumes larger than 500  $\mu\text{L}$ , otherwise engendering detrimental arcing in the superfluid helium bath (Vinther et al., 2019). Such scaling-up would be required for enabling parallel hyperpolarization of multiple transportable samples (Lipsø et al., 2017), and for volumes  $>1$  mL currently used for hyperpolarized human imaging (Nelson et al., 2013).

For hyperpolarizing larger sample volumes, alternative *rf*-sequences with reduced power requirements are desired. Lower power alternatives to CP have previously been described in the literature (Jeener et al., 1965; Jeener and Broekaert, 1967; Redfield, 1969; Kunitomo et al., 1974; Demco et al., 1975; Emid et al., 1980; Vieth and Yannoni, 1993; Zhang et al., 1993; Kurur and Bodenhausen, 1995; Lee and Khitritin, 2008; Khitritin et al., 2011; Vinther et al., 2019), which rely on indirect polarization transfer via proton dipolar order rather than through a direct  $^1\text{H}$ - $^{13}\text{C}$  Hartman-Hahn matching condition (Hartmann and Hahn, 1962).

The population of a Zeeman eigenstate for a spin-1/2 nucleus at thermal equilibrium  $\rho_{eq}^i$  is given as follows:

$$\rho_{eq}^i = \frac{\exp\left\{-\frac{\hbar\omega_i}{\kappa_B T}\right\}}{Z}, \quad (1)$$

where  $\omega_i$  is the energy of the state for the spin of interest,  $T$  is the temperature and  $Z$  is a canonical partition function. In the high-temperature limit, the spin density operator  $\hat{\rho}_{eq}$  (which describes the state of an entire ensemble of spin-1/2 nuclei at thermal equilibrium) is expressed by using a truncated Taylor series:

$$\hat{\rho}_{eq} \simeq \hat{1} + \mathbb{B} \sum_i \hat{I}_{iz}, \quad (2)$$

where  $\mathbb{B} = \hbar\omega_0/\kappa_B T$ ,  $\omega_0$  is the nuclear Larmor frequency for the spins of interest and  $\hat{I}_{iz}$  is  $z$ -angular momentum operator for spin  $i$ . The second term in Equation 2 corresponds to longitudinal magnetization. However, outside of the high-temperature approximation higher order terms in the spin density operator expansion cannot be ignored:

$$\hat{\rho}_{eq} \simeq \hat{1} + \mathbb{B} \sum_i \hat{I}_{iz} + \frac{\mathbb{B}^2}{2} \sum_i \sum_j \hat{I}_{iz} \cdot \hat{I}_{jz}. \quad (3)$$

The third term in Equation 3 reveals the presence of nuclear dipolar order (Fukushima and Roeder, 1981) which can in principle be prepared by generating strongly polarized spin systems, such as those established through conducting *d*DNP experiments (Sugishita et al., 2019). Such dipolar order can also be efficiently generated by suitable *rf*-pulse sequences, and ultimately used to transfer polarization (Jeener et al., 1965; Jeener and Broekaert, 1967; Redfield, 1969; Kunitomo et al., 1974; Demco et al., 1975; Emid et al., 1980; Vieth and Yannoni, 1993; Zhang et al., 1993; Kurur and Bodenhausen, 1995; Lee and Khitritin, 2008; Khitritin et al., 2011; Vinther et al., 2019). For the sake of simplicity, we will refer here to such polarization transfer schemes as *d*CP for dipolar order-mediated cross-polarization.

In this Article, we revisit the concept of  $^1\text{H} \rightarrow ^{13}\text{C}$  *d*CP polarization transfer and assess its efficiency in the context of *d*DNP experiments at 1.2 K and 7.05 T. We show that for a sample of  $[1-^{13}\text{C}]$ sodium acetate, a  $^{13}\text{C}$  polarization of  $\sim 8.7\%$  can be achieved after  $\sim 10$  minutes of  $^1\text{H}$  DNP and the use of a sole polarization transfer step. The overall *d*CP transfer efficiency is  $\sim 0.43$  with respect to the most sophisticated and efficient high power CP sequences available today. The experimental data presented indicate that  $^1\text{H}$  Zeeman order ( $\hat{I}_z$ ) is first converted to  $^1\text{H}$ - $^1\text{H}$  dipolar order ( $\hat{I}_{1z} \cdot \hat{I}_{2z}$ ) and presumably subsequently converted to the desired  $^{13}\text{C}$  Zeeman order ( $\hat{S}_z$ ). We show how the use of microwave gating (Bornet et al., 2016) is key to *d*CP as it improves the overall efficiency by a factor more than  $\sim 2.3$ .

## 2 Methods

88  
89  
90  
91  
92  
93  
94  
95  
96  
97  
98  
99  
00  
01  
02  
03  
04  
05  
06  
07  
08  
09  
10  
11  
12  
13  
14  
15  
16  
17  
18  
19

## 2.1 Sample Preparation and Freezing

A solution of 3 M [ $1\text{-}^{13}\text{C}$ ]sodium acetate in the glass-forming mixture  $\text{H}_2\text{O}:\text{D}_2\text{O}:\text{glycerol-}d_8$  (10%:30%:60% v/v/w) was doped with 50 mM TEMPOL radical (all compounds purchased from *Sigma Aldrich*) and sonicated for  $\sim 10$  minutes. This sample is referred to as **I** from here onwards. Paramagnetic TEMPOL radicals were chosen to most efficiently polarize  $^1\text{H}$  spins under *dDNP* conditions. A 100  $\mu\text{L}$  volume of **I** was pipetted into a Kel-F sample cup and inserted into a 7.05 T prototype *Bruker Biospin* polarizer equipped with a specialized *dDNP* probe and running *TopSpin 3.7* software. The sample temperature was reduced to 1.2 K by submerging the sample in liquid helium and reducing the pressure of the variable temperature insert (VTI) towards  $\sim 0.7$  mbar.

## 2.2 Dynamic Nuclear Polarization

The sample was polarized by applying microwave irradiation at 197.648 GHz (positive lobe of the EPR line) with triangular frequency modulation of amplitude  $\Delta f_{\text{mw}} = 120$  MHz (Bornet et al., 2014) and rate  $f_{\text{mod}} = 0.5$  kHz at a power of c.a. 100 mW, which were optimized prior to commencing experiments to achieve the best possible level of  $^1\text{H}$  polarization. Microwave gating was employed shortly before and during *dDNP* transfer experiments to allow the electron spin ensemble to return to a highly polarized state, which happens on the timescale of the longitudinal electron relaxation time (typically  $T_{1e} = 100$  ms with  $P_e = 99.93\%$  under *dDNP* conditions) (Bornet et al., 2016). Consequently, the  $^1\text{H}$  and  $^{13}\text{C}$  relaxation times in the presence of a *rf*-field are extended by orders of magnitude, allowing spin-locking *rf*-pulses to be much longer which significantly increases the efficiency of nuclear polarization transfer.

## 2.3 Pulse Sequences

In 1967 Jeener and Broekaert established the original *rf*-pulse sequence for creating and observing dipolar order in the solid-state (Jeener and Broekaert, 1967). Since then, other *rf*-pulse sequences have been proposed in the literature, usually with improved efficiency (Jeener et al., 1965; Redfield, 1969; Kunitomo et al., 1974; Demco et al., 1975; Emid et al., 1980; Vieth and Yannoni, 1993; Zhang et al., 1993; Kurur and Bodenhausen, 1995; Lee and Khitritin, 2008; Khitritin et al., 2011; Vinther et al., 2019). Herein, we are most interested in the *rf*-pulse sequence introduced by Vieth and Yannoni (Vieth and Yannoni, 1993) which is particularly simple, easily generates proton dipolar order and allows subsequent conversion to  $^{13}\text{C}$  polarization. Figure 1 shows this sequence adapted for our *dDNP* experiments. An electron-nuclear variant of this *rf*-pulse sequence has also been developed (Macho et al., 1991; Buntkowsky et al., 1991).

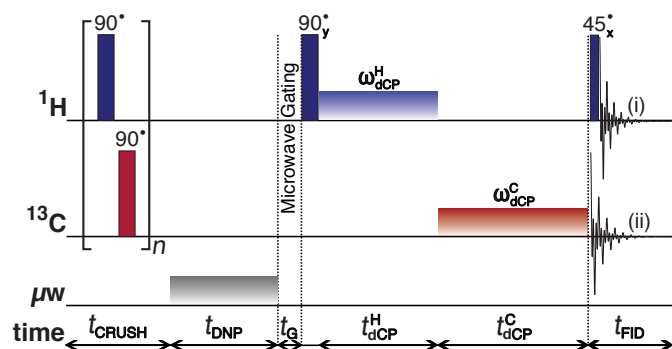


Figure 1: Schematic representation of the *dCP* *rf*-pulse sequence used for preparing and monitoring  $^1\text{H}$ - $^1\text{H}$  dipolar order in **I**, and the conversion to  $^{13}\text{C}$  transverse magnetization. The experiments used the following parameters, chosen to maximize magnetization-dipolar order interconversion:  $n = 250$ ;  $t_{\text{DNP}}$

24 = 5 s;  $t_G = 0.5$  s;  $\omega_{dCP}^H/2\pi = 16.4$  kHz;  $t_{dCP}^H = 25$   $\mu$ s;  $\omega_{dCP}^C/2\pi = 13.2$  kHz;  $t_{dCP}^C = 39$  ms. The  $^1\text{H}$  and  $^{13}\text{C}$  spin-locking *rf*-pulses have phase  $x$ . The  $\pi/2$  crusher  
25 *rf*-pulses use a thirteen-step phase cycle to remove residual magnetization at the beginning of each experiment:  $\{0, \pi/18, 5\pi/18, \pi/2, 4\pi/9, 5\pi/18, 8\pi/9,$   
26  $\pi, 10\pi/9, 13\pi/9, \pi/18, 5\pi/3, 35\pi/18\}$ . The resonance offset was placed at the centre of the  $^1\text{H}$  and  $^{13}\text{C}$  NMR peaks.

27

28 The *dCP* *rf*-pulse sequence operates as follows:

29 (i) A crusher sequence of  $90^\circ$  *rf*-pulses with alternating phases separated by a short delay (typically 11 ms) repeated  $n$  times  
30 (typically  $n = 250$ ) kills residual magnetization on both *rf*-channels;

31 (ii) The microwave source becomes active for a time  $t_{DNP}$  during which  $^1\text{H}$  DNP builds-up;

32 (iii) The microwave source is deactivated and a delay of duration  $t_G = 0.5$  s occurs before the next step, thus permitting the  
33 electron spins to relax to their highly polarized thermal equilibrium state (Bornet et al., 2016);

34 (iv) A  $^1\text{H}$   $90^\circ$  *rf*-pulse followed by a  $\pi/2$  phase-shifted spin-locking  $^1\text{H}$  *rf*-pulse of amplitude  $\omega_{dCP}^H$  and length  $t_{dCP}^H$  converts  $^1\text{H}$   
35 Zeeman polarization into  $^1\text{H}$ - $^1\text{H}$  dipolar order;

36 (v) A  $^{13}\text{C}$  square *rf*-pulse of amplitude  $\omega_{dCP}^C$  and length  $t_{dCP}^C$  presumably converts the  $^1\text{H}$ - $^1\text{H}$  dipolar order into  $^{13}\text{C}$  transverse  
37 magnetization.

38 The NMR signal can be detected by using either: (i) a  $^1\text{H}$   $45^\circ$  *rf*-pulse followed by  $^1\text{H}$  FID acquisition to monitor the remaining  
39 proton dipolar order; or (ii)  $^{13}\text{C}$  FID detection to observe the converted magnetization, see Figure 1.

40 The *dCP* *rf*-pulse sequence can be used in several variants:

41 *Variant #1*: Efficiency of  $^1\text{H}$ - $^1\text{H}$  dipolar order preparation.

42 (a)  $^1\text{H}$  observation by fixing  $t_{dCP}^C = 0$  ms and varying  $\omega_{dCP}^H$  and  $t_{dCP}^H$  (Figure 2a);

43 (b):  $^{13}\text{C}$  observation by fixing  $t_{dCP}^C$  and  $\omega_{dCP}^C$  (typically to an optimal value) and varying  $\omega_{dCP}^H$  and  $t_{dCP}^H$  (Figure 2c).

44 *Variant #2*: Efficiency of  $^1\text{H}$ - $^1\text{H}$  dipolar order conversion to  $^{13}\text{C}$  magnetization.

45 (a):  $^{13}\text{C}$  observation by fixing  $\omega_{dCP}^H$  and  $t_{dCP}^H$  (typically to an optimal value) and varying  $\omega_{dCP}^C$  and  $t_{dCP}^C$  (Figure 3a);

46 (b):  $^1\text{H}$  observation by fixing  $\omega_{dCP}^H$  and  $t_{dCP}^H$  (typically to an optimal value) and varying  $\omega_{dCP}^C$  and  $t_{dCP}^C$  (Figure 4a).

47 The amplitudes of the  $^1\text{H}$  and  $^{13}\text{C}$  *dCP* *rf*-pulses ( $\omega_{dCP}^H$  and  $\omega_{dCP}^C$ , respectively) were optimized iteratively until the intensity of  
48 the resulting NMR signals could not be improved further, see the Electronic Supplementary Material (ESM) for more details.

49 In the case of proton *rf*-channel acquisition, data points were acquired with a two-step phase cycle, in which the phase of the  
50  $90_y$  *rf*-pulse and the digitizer were simultaneously changed by  $180^\circ$  in successive transients, to remove spurious signals generated  
51 by longitudinal magnetization accrued during the *dCP* *rf*-pulses. A dispersive lineshape was observed as a result of the phase cycle,  
52 which is characteristic of dipolar spin order. The resulting  $^1\text{H}$  NMR spectrum was phase corrected to yield an absorptive lineshape.

53

## 54 3 Results

55

### 56 3.1 $^1\text{H}$ - $^1\text{H}$ Dipolar Order Preparation

57

58  $^1\text{H}$  monitored optimization for the generation of  $^1\text{H}$ - $^1\text{H}$  dipolar order as a function of the *dCP*  $^1\text{H}$  *rf*-pulse duration  $t_{dCP}^H$  was  
59 performed by using *variant #1a* of the *dCP* sequence shown in Figure 2a. Experimental results demonstrating the preparation of  
60  $^1\text{H}$ - $^1\text{H}$  dipolar order under *variant #1a* of the *dCP* sequence are shown in Figure 2b. The integrals plotted were acquired directly  
61 on the  $^1\text{H}$  *rf*-channel using  $\omega_{dCP}^H/2\pi = 16.4$  kHz either with or without microwave gating (black circles and grey squares,  
62 respectively). In both cases, the NMR signal grows until a maximum signal intensity, which corresponds to the optimal preparation  
63 of proton dipolar order, is reached at  $t_{dCP}^H \approx 25$   $\mu$ s, after which the signal decays towards a stable plateau on a longer timescale.  
64 However, in the case that microwave gating is removed, the signal intensity is reduced. This is due to depolarization (microwave  
65 saturation) of the electron spins, resulting in a detrimental enhancement of the paramagnetic relaxation contribution to nuclear spin

relaxation. These results suggest that microwave gating improves the conversion of  $^1\text{H}$  magnetization to  $^1\text{H}$ - $^1\text{H}$  dipolar order by a factor of at least  $\sim 1.6$ .

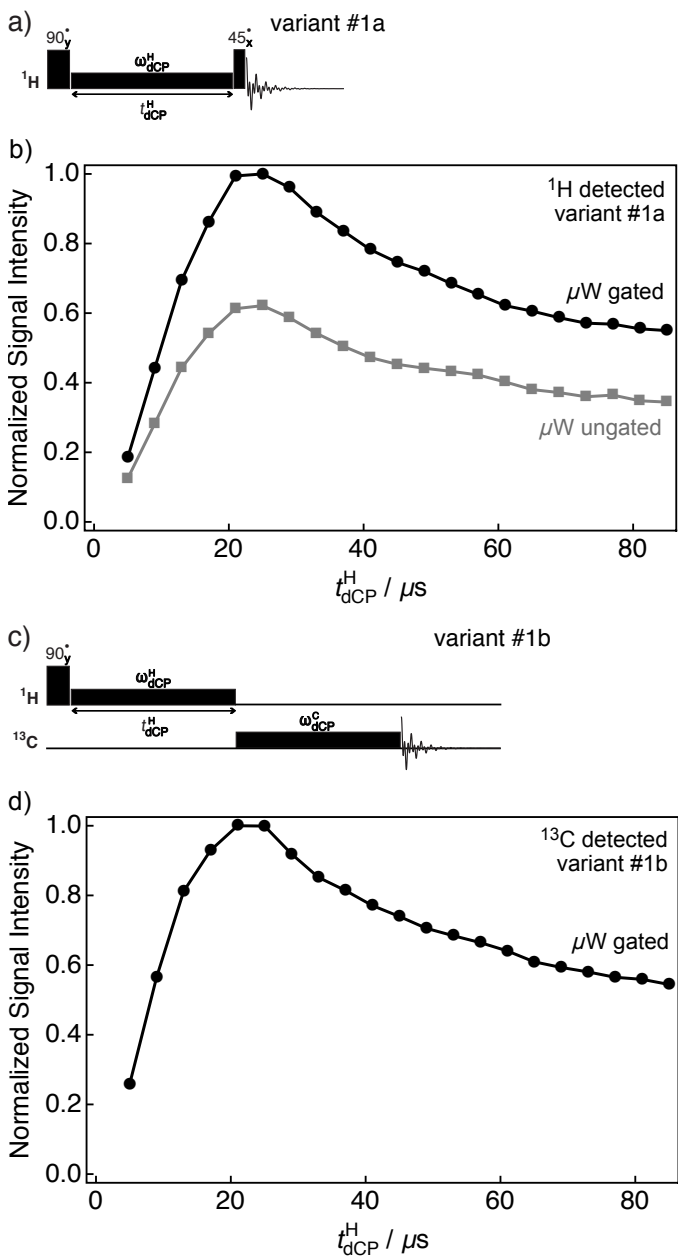


**Figure 2:** Simplified schematic representations of (a) *variant #1a* and (c) *variant #1b* of the *dCP* *rf*-pulse sequence. Experimental (b)  $^1\text{H}$  and (d)  $^{13}\text{C}$  NMR signal intensities of  $I$  as a function of the  $^1\text{H}$  *dCP* *rf*-pulse duration  $t_{\text{dCP}}^{\text{H}}$  acquired at 7.05 T ( $^1\text{H}$  nuclear Larmor frequency = 300.13 MHz,  $^{13}\text{C}$  nuclear Larmor frequency = 75.47 MHz) and 1.2 K. The experiments in (b) were acquired with two transients per data point, whilst the experiments in (d) were acquired with a single transient per data point. The traces have the same overall form, and plateau over a period of 200  $\mu\text{s}$  (data not shown).

$^{13}\text{C}$  monitored optimization for the build-up of  $^1\text{H}$ - $^1\text{H}$  dipolar order was performed by using *variant #1b* of the *dCP* *rf*-pulse sequence demonstrated in Figure 2c. In Figure 2d the experimental integrals are plotted against the *dCP*  $^1\text{H}$  *rf*-pulse duration  $t_{\text{dCP}}^{\text{H}}$  and were acquired on the  $^{13}\text{C}$  *rf*-channel with  $\omega_{\text{dCP}}^{\text{H}}/2\pi = 16.4$  kHz,  $\omega_{\text{dCP}}^{\text{C}}/2\pi = 13.2$  kHz and  $t_{\text{dCP}}^{\text{C}} = 39$  ms (black circles). It is important to note that the maximum is identical whether the NMR signal is observed on the  $^1\text{H}$  *rf*-channel by using *variant #1a* or on the  $^{13}\text{C}$  *rf*-channel by using *variant #1b*, and more generally that the two traces have the same shape and optimum. This shows that  $^{13}\text{C}$  transverse magnetization from *dCP* is proportional to the  $^1\text{H}$ - $^1\text{H}$  dipolar order initially prepared.

### 3.2 $^1\text{H}$ - $^{13}\text{C}$ Polarization Transfer

Figure 3b shows how  $^{13}\text{C}$  magnetization is built-up by employing *variant #2a* the  $d\text{CP}$   $rf$ -pulse sequence, see Figure 3a. The experimental integrals of the  $^{13}\text{C}$  signal are plotted against the  $^{13}\text{C}$   $d\text{CP}$   $rf$ -pulse duration  $t_{\text{dCP}}^{\text{C}}$  with (black circles) and without (grey squares) microwave gating.

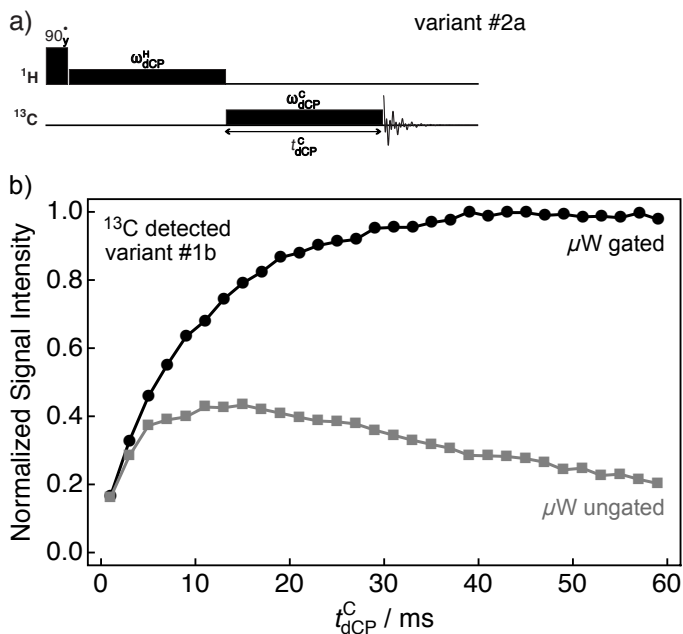
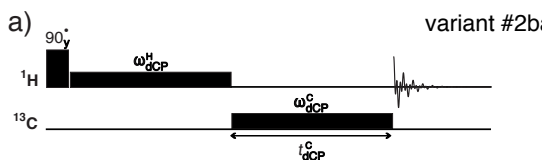


**Figure 3:** (a) Simplified schematic representation of *variant #2a* of the  $d\text{CP}$   $rf$ -pulse sequence. (b) Experimental  $^{13}\text{C}$  NMR signal intensity of  $I$  as a function of the  $d\text{CP}$   $rf$ -pulse duration  $t_{\text{dCP}}^{\text{C}}$  acquired at 7.05 T ( $^1\text{H}$  nuclear Larmor frequency = 300.13 MHz,  $^{13}\text{C}$  nuclear Larmor frequency = 75.47 MHz) and 1.2 K with a single transient per data point.

The black trace corresponds to the growth of the  $^{13}\text{C}$  NMR signal. A maximum is reached at  $t_{\text{dCP}}^{\text{C}} \approx 39$  ms, with  $\omega_{\text{dCP}}^{\text{C}} = 13.2$  kHz. The polarization transfer efficiency is relatively robust with respect to the amplitude of the  $^{13}\text{C}$   $d\text{CP}$   $rf$ -pulse  $\omega_{\text{dCP}}^{\text{C}}$ , see the ESM for more details. A wildly different behaviour is observed in the case where the microwave source is not gated. In this instance, a maximum signal intensity occurs at  $t_{\text{dCP}}^{\text{C}} \approx 15$  ms, with the detectable  $^{13}\text{C}$  signal decreasing past this point. The ratio between the maximum data points is  $\sim 2.3$ , and indicates a large  $^{13}\text{C}$  enhancement afforded by microwave gating.

It is worth noting that the duration of the  $^{13}\text{C}$   $d\text{CP}$   $rf$ -pulse is considerably longer, more than three orders of magnitude, than the  $^1\text{H}$   $d\text{CP}$   $rf$ -pulse lengths. Reasons for this are examined in the discussion section below.

Figure 4b details how in *variant #2b* of the  $d\text{CP}$   $rf$ -pulse sequence (Figure 4a) the  $^1\text{H}$  NMR signal vanishes as the  $^{13}\text{C}$   $d\text{CP}$   $rf$ -pulse generates  $^{13}\text{C}$  transverse magnetization. The experimental integrals of the  $^1\text{H}$  detected NMR signals are plotted against the  $^{13}\text{C}$   $d\text{CP}$   $rf$ -pulse duration  $t_{\text{dCP}}^{\text{C}}$  with  $\omega_{\text{dCP}}^{\text{C}} = 0$  kHz (black open circles) and  $\omega_{\text{dCP}}^{\text{C}} = 13.2$  kHz (black circles) both with microwave gating, and with  $\omega_{\text{dCP}}^{\text{C}} = 13.2$  kHz (grey squares) without microwave gating.



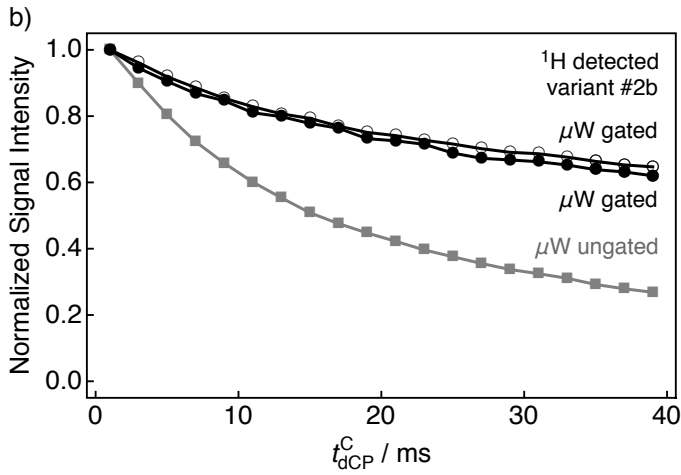


Figure 4: (a) Simplified schematic representation of *variant #2b* of the *dCP rf-pulse* sequence. (b) Experimental  $^1\text{H}$  NMR signal intensity of I as a function of the  $^{13}\text{C}$  *dCP rf-pulse* duration  $t_{dCP}^C$  acquired at 7.05 T ( $^1\text{H}$  nuclear Larmor frequency = 300.13 MHz,  $^{13}\text{C}$  nuclear Larmor frequency = 75.47 MHz) and 1.2 K with two transients per data point. The experimental traces were recorded by using the following amplitudes for the  $^{13}\text{C}$  *dCP rf-pulse*  $\omega_{dCP}^C$ : Black open circles:  $\omega_{dCP}^C = 0$  kHz; Black filled circles:  $\omega_{dCP}^C = 13.2$  kHz; Grey squares:  $\omega_{dCP}^C = 13.2$  kHz. All signal amplitudes were normalized to the first data point.

The curves show how  $^1\text{H}$ - $^1\text{H}$  dipolar order decays towards thermal equilibrium mainly through relaxation and is not significantly affected by the presence of the  $^{13}\text{C}$  *dCP rf-pulse* generating  $^{13}\text{C}$  magnetization. The difference between the two black traces might however indicate the quantity of  $^1\text{H}$ - $^1\text{H}$  dipolar order converted into  $^{13}\text{C}$  magnetization. The small difference is just a few percent, indicating that only a very small portion of the  $^1\text{H}$ - $^1\text{H}$  dipolar order might be used (and be useful) to produce hyperpolarized  $^{13}\text{C}$  magnetization. This could be explained by the large excess of  $^1\text{H}$  spins compared with  $^{13}\text{C}$  spins in our sample (a factor of  $\sim 6.2$ ). A lack of microwave gating (grey squares) significantly compromises the generation of  $^{13}\text{C}$  polarization, as seen in Figure 3b.

### 3.3 Comparison to Cross-Polarization

The performance efficiency of the *dCP rf-pulse* sequence was compared to a traditional CP experiment (Hartmann and Hahn, 1962; Pines et al., 1972; Perez Linde, 2009; Jannin et al., 2011; Bornet et al., 2012; Batel et al., 2012; Bornet et al., 2013; Vuichoud et al., 2016; Cavaillès et al., 2018), which is described in the ESM along with a *rf-pulse* sequence diagram and all optimized parameters. Experiments employed 640 s of direct  $^1\text{H}$  DNP at 1.2 K prior to polarization transfer to the  $^{13}\text{C}$  heteronucleus.

The power requirements for polarization transfer are dependent upon the *rf-pulse* sequence used and the capabilities of the *dDNP* probe. In general, the peak power for the  $^{13}\text{C}$  *dCP rf-pulse* is  $\sim 5.4$  times lower than required for CP. However, the  $^{13}\text{C}$  *dCP rf-pulse* is active for a duration  $\sim 5.6$  times longer than that of CP, and hence the overall deposited *rf-pulse* energy is approximately the same for both *rf-pulse* sequences. Notwithstanding, the moderately lower  $^{13}\text{C}$  *dCP rf-pulse* power is highly advantageous, e.g. decreased likelihood of probe arcing events within the superfluid helium bath. The benefit of employing the *dCP rf-pulse* sequence becomes even more apparent when examining the proton *rf-pulse* durations needed for  $^1\text{H}$ - $^{13}\text{C}$  polarization transfer. Although the peak powers of both *rf-pulse* sequences are similar, the duration of the  $^1\text{H}$  *dCP rf-pulse* is a factor of 280 times shorter than that recommended for adequate CP. This is advantageous in the case that the  $B_1$ -field produced by the *dDNP* probe is weak (e.g. due to large sample constraints) or is unstable at higher  $^1\text{H}$  *rf-pulse* powers for sufficiently long durations.

The CP *rf-pulse* sequence achieved a  $^{13}\text{C}$  polarization level of  $P(^{13}\text{C}) \approx 20.4\%$  after a single CP contact.  $^{13}\text{C}$  polarization levels in excess of 60% are anticipated by using a multiple CP contact approach (Perez Linde, 2009; Jannin et al., 2011; Bornet et al., 2012; Batel et al., 2012; Bornet et al., 2013; Vuichoud et al., 2016; Cavaillès et al., 2018). In comparison, the integral of the *dCP*-filtered NMR signal maximum is scaled by a factor of  $\sim 0.43$ , indicating a  $^{13}\text{C}$  polarization of  $P(^{13}\text{C}) \approx 8.7\%$ . This is consistent

with previous results reported in the literature (Perez Linde, 2009; Vinther et al., 2019). Strategies to further improve the *dCP* efficiency are presented in the discussion section.

#### 4 Discussion

The results presented in Figure 2b and Figure 2d show how the achieved  $^{13}\text{C}$  polarization is directly proportional to the quantity of  $^1\text{H}$ - $^1\text{H}$  dipolar order initially prepared by the  $^1\text{H}$  *dCP* *rf*-pulse. However, even if the  $^{13}\text{C}$  polarization closely follows the shape of the proton dipolar order creation profile, this does not constitute irrefutable proof that the  $^{13}\text{C}$  polarization originates from the proton dipolar order reservoir itself. Other, more-complex forms of nuclear spin order might be involved. Moreover, it is feasible that an intermediate reservoir exists, such as non-Zeeman spin order of the  $^{13}\text{C}$  heteronucleus.

As seen in Figure 3b, it is interesting to note that the duration of the  $^{13}\text{C}$  *dCP* *rf*-pulse is considerably longer, more than three orders of magnitude, than the  $^1\text{H}$  *dCP* *rf*-pulse duration. The reason is the relative sizes of the dipolar couplings which control the preparation and transfer processes of  $^1\text{H}$ - $^1\text{H}$  dipolar order. The generation of dipolar order involves only proton spins, which possess a magnetogyric ratio  $\sim 4$  times greater than for  $^{13}\text{C}$  spins and consequently larger dipolar couplings, which scale as the product of the magnetogyric ratios for the two spins involved. This results in a short time to convert  $^1\text{H}$  magnetization to  $^1\text{H}$ - $^1\text{H}$  dipolar order. Conversely, the supposed transfer of  $^1\text{H}$ - $^1\text{H}$  dipolar order to  $^{13}\text{C}$  nuclei would certainly demand  $^1\text{H}$ - $^{13}\text{C}$  dipolar couplings.

The duration of the  $^{13}\text{C}$  *dCP* *rf*-pulse is a factor of  $\sim 5.6$  longer than required for optimized conventional CP (see the ESM for more details). The extended duration of the  $^{13}\text{C}$  *dCP* *rf*-pulse could be conceivably explained by assuming that the  $^1\text{H}$  spins closest to the  $^{13}\text{C}$  spin do not participate in the polarization transfer process since the  $^1\text{H}$ - $^1\text{H}$  dipolar order preparation is perturbed by the presence of the  $^{13}\text{C}$  spin during the  $^1\text{H}$  *dCP* *rf*-pulse. It is also possible that two dipolar coupled protons are separated by a difference in chemical shift which matches the frequency of a  $^{13}\text{C}$  spin the rotating frame allowing an exchange of energy. Such events are similar to the cross-effect in DNP (Kessenikh et al., 1963) but are likely to be of lower probability, leading to an increased  $^{13}\text{C}$  *dCP* *rf*-pulse duration.

Not only is the polarization transfer process long, but it is also weaker than what is usually realized with optimized CP, since we obtain  $P(^{13}\text{C}) \approx 8.7\%$  rather than  $P(^{13}\text{C}) \approx 20.4\%$  in a single CP step on the same sample. Although the amplitude  $\omega_{\text{dCP}}^{\text{H}}$  and duration  $t_{\text{dCP}}^{\text{H}}$  of the proton dipolar order creation *rf*-pulse were carefully optimized before experimental implementation, we nevertheless believe there is still room for improvement in preparing high quantities of proton dipolar order. The performance of the *dCP* *rf*-pulse sequence could be enhanced by adopting the following strategies: (i) employing shaped *rf*-pulses; (ii) implementing a multiple *dCP* transfer approach; (iii) optimizing the protonation level of the DNP glassing solution; (iv) exploiting deuterated molecular derivatives; (v) avoiding large quantities of methyl groups which may act as dipolar order relaxation sinks due to their inherent rotation (which remains present at liquid helium temperature); and (vi) changing the molecule [ $1\text{-}^{13}\text{C}$ ]sodium acetate for another spin system with different  $^1\text{H}$ - $^{13}\text{C}$  coupling strengths (e.g. simply using [ $2\text{-}^{13}\text{C}$ ]sodium acetate).

Today's performances on our current 'standard' DNP sample are rather poor compared to CP, however, there are reasons to think that further improvements through advanced *rf*-pulse schemes and revised sample formulations will be possible in the future, and that *dCP* may become a viable alternative to CP. This will be particularly relevant to the cases of: (i) issues related to probe arcing in the superfluid helium bath which precludes the use of conventional CP experiments; (ii) increased sample volumes, e.g. in human applications; and (iii) hyperpolarization of insensitive nuclear spins, e.g.  $^{89}\text{Y}$  nuclei cannot be polarized easily via traditional CP experiments due to unfeasible CP matching conditions on the heteronuclear *rf*-channel. Other alternatives to the CP approach also exist but are theoretically less efficient, such as low magnetic field nuclear thermal mixing (Gadian et al., 2012) which relies on energy conserving mutual spin-flips in overlapping NMR lineshapes to polarize heteronuclei in solid samples (Peat et al., 2016).



## 38 5 Conclusions

39

40  $^1\text{H}\rightarrow^{13}\text{C}$  polarization transfer occurs by employing *rf*-pulse methods which operate under *d*DNP conditions. This supposedly  
41 involves an intermediate reservoir of dipolar order, which governs the polarization transfer process. The spin dynamics of dipolar  
42 order mediated cross-polarization (*d*CP) were found to significantly depend on the presence of microwave gating. A maximum  $^{13}\text{C}$   
43 polarization of  $\sim 8.7\%$  was observed after  $\sim 10$  minutes of microwave irradiation and a lone polarization step, which corresponds to  
44 a *d*CP polarization transfer efficiency of  $\sim 0.43$  with respect to optimized conventional CP. These results are promising for future  
45 applications of polarization conversion methods in the context of low power  $^1\text{H}\rightarrow\text{X}$  polarization transfer to insensitive nuclei (in  
46 particular for very low magnetogyric ratios), with minimized probe arcing and potentially large sample volumes, paving the way  
47 to the use of  $^1\text{H}\rightarrow\text{X}$  polarization transfer in clinical (human-dose) contexts.

48

## 49 Acknowledgements

50

51 The authors gratefully acknowledge *Bruker Biospin* for providing the prototype *d*DNP polarizer, and particularly Dmitry  
52 Eshchenko, Roberto Melzi, Marc Rossire, Marco Sacher and James Kempf for scientific and technical support. The authors  
53 additionally acknowledge Gerd Buntkowsky (Technische Universitat Darmstadt) who kindly communicated data associated with  
54 prior publications to us; Burkhard Luy (Karlsruhe Institute of Technology) for enlightening discussions; Catherine Jose and  
55 Christophe Pages for use of the ISA Prototype Service; and Stéphane Martinez of the UCBL mechanical workshop for machining  
56 parts of the experimental apparatus.

57

## 58 Financial Support

59

60 This research was supported by ENS-Lyon, the French CNRS, Lyon 1 University, the European Research Council under the  
61 European Union's Horizon 2020 research and innovation program (ERC Grant Agreements No. 714519 / HP4all and Marie  
62 Skłodowska-Curie Grant Agreement No. 766402 / ZULF).

63

## 64 Author Contributions

65

66 SJE performed experiments and co-wrote the manuscript, SFC/QC/OC/AB performed experiments, MC built parts of the  
67 experimental apparatus, and SJ conceived the idea and co-wrote the manuscript.

68

## 69 Competing Interests

70

71 The authors declare no competing interests.

72

## 73 References

74

- 75 Ardenkjær-Larsen, J.-H., Fridlund, B., Gram, A., Hansson, G., Hansson, L., Lerche, M. H., Servin, R., Thaning, M., and Golman, K.: Increase in signal-to-noise  
76 ratio of  $> 10,000$  times in liquid-state NMR, *Proc. Natl. Acad. Sci. U.S.A.*, 100, 10158-10163, <https://doi.org/10.1073/pnas.1733835100>, 2003.
- 77 Bornet, A., Ji, X., Mammoli, D., Vuichoud, B., Milani, J., Bodenhausen, G., and Jannin, S.: Long-Lived States of Magnetically Equivalent Spins Populated by  
78 Dissolution-DNP and Revealed by Enzymatic Reactions, *Chem.: Eur. J.*, 20, 17113-17118, <https://doi.org/10.1002/chem.201404967>, 2014.
- 79 Dumez, J.-N., Milani, J., Vuichoud, B., Bornet, A., Lalande-Martin, J., Tea, I., Yon, M., Maucourt, M., Deborde, C., Moing, A., Frydman, L., Bodenhausen, G.,  
80 Jannin, S., and Giraudeau, P.: Hyperpolarized NMR of plant and cancer cell extracts at natural abundance, *Analyst*, 140, 5860-5863,  
81 <https://doi.org/10.1039/C5AN01203A>, 2015.

32 Bornet, A., Maucourt, M., Deborde, C., Jacob, D., Milani, J., Vuichoud, B., Ji, X., Dumez, J.-N., Moing, A., Bodenhausen, G., Jannin, S., and Giraudeau, P.: Highly  
33 Repeatable Dissolution Dynamic Nuclear Polarization for Heteronuclear NMR Metabolomics, *Anal. Chem.*, 88, 6179-6183,  
34 <https://doi.org/10.1021/acs.analchem.6b01094>, 2016.

35 Hartmann, G., Hubert, D., Mango, S., Morehouse, C. C., and Plog, K.: Proton polarization in alcohols at 50 kG, 1 K, *Nucl. Instrum. Meth. A*, 106, 9-12,  
36 [https://doi.org/10.1016/0029-554X\(73\)90039-6](https://doi.org/10.1016/0029-554X(73)90039-6), 1973.

37 Hartmann, S. R., and Hahn, E. L.: Nuclear Double Resonance in the Rotating Frame, *Phys. Rev.*, 128, 204-2053, <https://doi.org/10.1103/PhysRev.128.2042>, 1962.

38 Pines, A., Gibby, M., and Waugh, J.: Proton-enhanced nuclear induction spectroscopy <sup>13</sup>C chemical shielding anisotropy in some organic solids, *Chem. Phys. Lett.*,  
39 15, 373-376, [https://doi.org/10.1016/0009-2614\(72\)80191-X](https://doi.org/10.1016/0009-2614(72)80191-X), 1972.

40 Perez Linde, A. J.: Application of Cross-Polarization Techniques to Dynamic Nuclear Polarisation Dissolution Experiments, PhD Thesis, University of Nottingham,  
41 UK, 2009.

42 Jannin, S., Bornet, A., Colombo, S., and Bodenhausen, G.: Low-temperature cross polarization in view of enhancing dissolution Dynamic Nuclear Polarization in  
43 NMR, *Chem. Phys. Lett.*, 517, 234-236, <https://doi.org/10.1016/j.cplett.2011.10.042>, 2011.

44 Bornet, A., Melzi, R., Jannin, S., and Bodenhausen, G.: Cross Polarization for Dissolution Dynamic Nuclear Polarization Experiments at Readily Accessible  
45 Temperatures  $1.2 < T < 4.2$ , *Appl. Magn. Reson.*, 43, 107-117, <https://doi.org/10.1007/s00723-012-0358-1>, 2012.

46 Batel, M., Krajewski, M., Däpp, A., Hunkeler, A., Meier, B. H., Kozerke, S., and Ernst, M.: Cross-Polarization for dissolution dynamics nuclear polarization,  
47 *Chem. Phys. Lett.*, 554, 72-76, <https://doi.org/10.1039/C4CP02696A>, 2012.

48 Bornet, A., Melzi, R., Perez Linde, A. J., Hautle, P., van den Brandt, B., Jannin S., and Bodenhausen, G.: Boosting Dissolution Dynamic Nuclear Polarization by  
49 Cross Polarization, *J. Chem. Phys. Lett.*, 4, 111-114, <https://doi.org/10.1021/jz301781t>, 2013.

50 Vuichoud, B., Bornet, A., de Nanteuil, F., Milani, J., Canet, E., Ji, X., Miéville, P., Weber, E., Kurzbach, D., Flamm, A., Konrat, R., Gossert, A. D., Jannin, S., and  
51 Bodenhausen, G.: Filterable Agents for Hyperpolarization of Water, Metabolites, and Proteins, *Chem.: Eur. J.*, 22, 14696-14700,  
52 <https://doi.org/10.1002/chem.201602506>, 2016.

53 Cavallès, M., Bornet, A., Jaurand, X., Vuichoud, B., Baudouin, D., Baudin, M., Veyre, L., Bodenhausen, G., Dumez, J.-N., Jannin, S., Copéret, C., and Thieuleux,  
54 C.: Tailored Microstructured Hyperpolarizing Matrices for Optimal Magnetic Resonance Imaging, *Angew. Chem. Int. Ed.*, 130, 7575-7579,  
55 <https://doi.org/10.1002/anie.201801009>, 2018.

56 Ji, X., Bornet, A., Vuichoud, B., Milani, J., Gajan, D., Rossini, A. J., Emsley, L., Bodenhausen, G., and Jannin, S.: Transportable Hyperpolarized Metabolites, *Nat.*  
57 *Commun.*, 8, 13975, <https://doi.org/10.1038/ncomms13975>, 2017.

58 Vinther, J. M. O., Zhurbenko, V., Albannay, M. M., and Ardenkjær-Larsen, J.-H.: Design of a local quasi-distributed tuning and matching circuit for dissolution  
59 DNP cross polarization, *Solid State Nucl. Mag.*, 102, 12-20, <https://doi.org/10.1016/j.ssnmr.2019.04.006>, 2019.

60 Lipsø, K. W., Bowen, S., Rybalko, O., and Ardenkjær-Larsen, J.-H.: Large dose hyperpolarized water with dissolution-DNP at high magnetic field, *J. Magn. Reson.*,  
61 274, 65-72, <https://doi.org/10.1016/j.jmr.2016.11.008>, 2017.

62 Nelson, S. J., Kurhanewicz, J., Vigneron, D. B., Larson, P. E. Z., Harzstark, A. L., Ferrone, M., van Criekinge, M., Chang, J. W., Bok, R., Park, I., Reed, G.,  
63 Carvajal, L., Small, E. J., Munster, P., Weinberg, V. K., Ardenkjær-Larsen, J.-H., Chen, A. P., Hurd, R. E., Odegardstuen, L.-I., Robb, F. J., Tropp, J., and Murray,  
64 J. A.: Metabolic imaging of patients with prostate cancer using hyperpolarized [<sup>13</sup>C]pyruvate, *Sci. Trans. Med.*, 5, 198ra108,  
65 <https://doi.org/10.1126/scitranslmed.3006070>, 2013.

66 Jeener, J., Du Bois, R., and Broekaert, P.: "Zeeman" and "Dipolar" Spin Temperatures during a Strong rf Irradiation, *Phys. Rev.*, 139, A1959-A1961,  
67 <https://doi.org/10.1103/PhysRev.139.A1959>, 1965.

68 Jeener, J., and Broekaert, P.: Nuclear Magnetic Resonance in Solids: Thermodynamic Effects of a Pair of rf Pulses, *Phys. Rev.*, 157, 232-240,  
69 <https://doi.org/10.1103/PhysRev.157.232>, 1967.

70 Redfield, A. G.: Nuclear spin thermodynamics in the rotating frame, *Science*, 164, 1015-1023, <https://doi.org/10.1126/science.164.3883.1015>, 1969.

71 Kunitomo, M., Hatanaka, H., and Hashi, T.: Adiabatic demagnetization in the rotating frame by non-resonant oscillating field, *Phys. Lett. A*, 49, 135-136,  
72 [https://doi.org/10.1016/0375-9601\(74\)90705-1](https://doi.org/10.1016/0375-9601(74)90705-1), 1974.

73 Demco, D. E., Tegenfeldt, J., and Waugh, J. S.: Dynamics of cross relaxation in nuclear magnetic double resonance, *Phys. Rev. B*, 11, 4133-4151,  
74 <https://doi.org/10.1103/PhysRevB.11.4133>, 1975.

75 Emid, S., Konijnendijk, J., Smidt, J., and Pines, A.: On the short time behavior of the dipolar signal in relaxation measurements by the pulse method, *Physica B+C*,  
76 100, 215-218, [https://doi.org/10.1016/0378-4363\(80\)90008-X](https://doi.org/10.1016/0378-4363(80)90008-X), 1980.

77 Vieth, H.-M., and Yannoni, C. S.: Cross polarization in solid state NMR spectroscopy. Efficient polarization transfer via the non-Zeeman spin reservoir, *Chem.*  
78 *Phys. Lett.*, 205, 153-156, [https://doi.org/10.1016/0009-2614\(93\)89220-C](https://doi.org/10.1016/0009-2614(93)89220-C), 1993.

79 Zhang, S., Stejskal, E., Fornes, R., and Wu, X.: Mismatching Cross Polarization in the Rotating Frame, *J. Magn. Reson., Ser A*, 104, 177-179,  
80 <https://doi.org/10.1006/jmra.1993.1206>, 1993.

81 Kurur, N. D., and Bodenhausen, G.: Adiabatic Coherence Transfer in Magnetic Resonance of Homonuclear Scalar-Coupled Systems, *J. Magn. Reson. A*, 114, 163-  
82 173, <https://doi.org/10.1006/jmra.1995.1123>, 1995.

83 Lee, J.-S., and Khitrin, A. K.: Thermodynamics of adiabatic cross polarization, *J. Chem. Phys.*, 128, 114504, <https://doi.org/10.1063/1.2839436>, 2008.

84 Khitrin, A. K., Xu, J., and Ramamoorthy, A.: Cross-correlations between low- $\gamma$  nuclei in solids via a common dipolar bath, *J. Magn. Reson.*, 212, 95-101,  
85 <https://doi.org/10.1016/j.jmr.2011.06.015>, 2011.  
86 Fukushima, E., and Roeder, S. B. W.: *Experimental Pulse NMR: A Nuts and Bolts Approach*, CRC Press, Boca Raton, 1981.  
87 Sugishita, T., Matsuki, Y., and Fujiwara, T.: Absolute  $^1\text{H}$  polarization measurement with a spin-correlated component of magnetization by hyperpolarized MAS-  
88 DNP solid-state NMR, *J. Magn. Reson.*, 99, 20-26, <https://doi.org/10.1016/j.ssnmr.2019.02.001>, 2019.  
89 Bornet, A., Pinon, A., Jhahharia, A., Baudin, M., Ji, X., Emsley, L., Bodenhausen, G., Ardenkjær-Larsen, J.-H., and Jannin, S.: Microwave-gated dynamic nuclear  
90 polarization, *Phys. Chem. Chem. Phys.*, 18, 30530-30535, <https://doi.org/10.1039/C6CP05587G>, 2016.  
91 Bornet, A., Milani, J., Vuichoud, B., Perez Linde, A. J., Bodenhausen, G., and Jannin, S.: Microwave frequency modulation to enhance Dissolution Dynamic  
92 Nuclear Polarization, *Chem. Phys. Lett.*, 602, 63-67, <https://doi.org/10.1016/j.cplett.2014.04.013>, 2014.  
93 Macho, V., Stehlik, D., and Vieth, H.-M.: Spin coherence effects in the electron-nuclear polarization transfer process, *Chem. Phys. Lett.*, 180, 398-402,  
94 [https://doi.org/10.1016/0009-2614\(91\)85139-N](https://doi.org/10.1016/0009-2614(91)85139-N), 1991.  
95 Buntkowsky, G., Stehlik, D., Vieth, H.-M., and Salikhov, K.M.: Nanosecond time resolution of electron-nuclear cross polarization within the optical nuclear  
96 polarization (ONP) process, *J. Phys.: Condens Matter*, 3, 6093-6111, <https://doi.org/10.1088/0953-8984/3/32/015>, 1991.  
97 Kessenikh, A. V., Lushchikov, V. I., Manenkov, A. A., and Taran, Y. V., *Sov. Phys. Solid State*, 5, 321-329, 1963.  
98 Gadian, D. G., Panesar, K. S., Perez Linde, A. J., Horsewill, A. J., Köckenberger, W., and Owers-Bradley, J. R.: Preparation of highly polarized nuclear spin  
99 systems using brute-force and low-field thermal mixing, *Phys. Chem. Chem. Phys.*, 14, 5397-5402, <https://doi.org/10.1039/C2CP23536F>, 2012.  
00 Peat, D. T., Hirsch, M. L., Gadian, D. G., Horsewill, A. J., Owers-Bradley, J. R., and Kempf, J. G.: Low-field thermal mixing in [ $^{13}\text{C}$ ] pyruvic acid for brute-  
01 force hyperpolarization, *Phys. Chem. Chem. Phys.*, 18, 19173-19182, <https://doi.org/10.1039/C6CP02853E>, 2016.  
02

### 03 **Response to Referee 1 Comment**

04

05 The manuscript entitled "Dipolar Order Mediated  $^1\text{H} \rightarrow ^{13}\text{C}$  Cross-Polarization for Dissolution-Dynamic Nuclear Polarization"  
06 by Stuart J. Elliott et al. entails a discussion of an alternative way, apart from the Hartmann-Hahn cross-polarization method, to  
07 harness the high nuclear polarization of hyperpolarized  $^1\text{H}$  spins and transfer it to  $^{13}\text{C}$  spins via simpler, low-power and non-  
08 synchronized  $^1\text{H}$  and  $^{13}\text{C}$  *rf*-pulses.  
09

10

11 In my opinion, the experimental demonstration of  $^1\text{H}$  to  $^{13}\text{C}$  polarization transfer mediated by dipolar order is certainly a  
12 welcome addition to the technical developments in (dissolution-dynamic nuclear polarization *d*DNP), in pursuit of simpler  
13 alternative to DNP cross polarization in terms of *rf*-hardware and *rf*-pulses. One of the main advantages of this reported technique  
14 is the use of non-simultaneous  $^1\text{H}$  and  $^{13}\text{C}$  *rf*-pulses in the DNP polarization transfer. This reported technique also opens up an  
15 avenue for polarizing larger DNP sample volumes with minimal probe arcing. For these and other reasons, I believe that this  
16 manuscript is significant in terms of scientific content and it brings some new technical insights to the magnetic resonance  
17 community, in particular to the rapidly growing *d*DNP field. Therefore, I would like to recommend publication of this manuscript  
18 with minor revision addressing the following suggestions and comments:  
19

20

21 The author response is given in italics.

22

23 (Q1) Page 1: In the title, should it be "Dipolar Order-Mediated..." with the dash? (Q2) Page 1: lines 37 and 43—please spell out  
24 "typ." to typically. (Q3) Page 4: line 26—same comment as #2. (Q4) page 4: line 29—should be "the microwave is deactivated" (Q5)  
25 Page 7: Figure 4 caption, line 17—"nuclear Larmor frequency" was used twice; I suggest to use symbol omega or make it concise.

26

27 (A1) *The authors have changed the title. (A2,A3) These changes have been made throughout the manuscript. (A4) The spelling has been corrected. (A5) The authors will stick to the current notation in order to be consistent throughout the manuscript.*

28 (Q6) The authors mentioned that this dipolar order-mediated CP technique (~8.7%) is only about a half as efficient compared  
29 to the conventional CP-DNP technique (~20.4%) in terms of the final  $^{13}\text{C}$  DNP-enhanced polarization obtained. Do the authors  
30 have a  $^{13}\text{C}$  polarization value for direct  $^{13}\text{C}$  polarization (without CP or dipolar order CP) of this sample?  
31

32 *(A6) The  $^{13}\text{C}$  nuclear polarization level for direct DNP was unfortunately not recorded for this sample because it is inefficient  
33 and displays a very long build-up time.*

34  
35 (Q7) I assume these numbers (~8.7% for dipolar-order CP, ~20.4% for conventional CP) are solid-state  $^{13}\text{C}$  polarizations. Do  
36 the authors have liquid-state  $^{13}\text{C}$  polarization numbers (post dissolution)? These are not a requirement for this paper, but I think it  
37 would be good to report them if the data are available.  
38

39 *(A7) The  $^{13}\text{C}$  nuclear polarization values presented were measured in the solid-state. Liquid state  $^{13}\text{C}$  polarization levels (post  
40 dissolution) could be measured in the future and be presented as part of a separate publication.*

41  
42 (Q8) Obviously there's a lot of optimization to be done here in this preliminary technical report especially with DNP sample  
43 optimization. Can the authors expand on the possible effects of the efficiency of dipolar order-mediated CP if the  $^1\text{H}$  spin density  
44 is increased or decreased in the glassing matrix?  
45

46 *(A8) Upon increasing the  $^1\text{H}$  spin density within the glassing matrix, an improvement is observed in the performance of the  
47 dCP rf-pulse sequence with respect to that of a sophisticated and high rf-power CP experiment.*

#### 48 49 **Response to Referee 2 Comment**

50  
51 Following the introduction of dissolution-DNP (dDNP) by Golman and Ardenkjær-Larsen, there have been discussions of  
52 approaches to shorten the hours long times required for the  $e^- \rightarrow ^{13}\text{C}$  polarization transfer process. This step is limited by the slow  
53  $^{13}\text{C}$ - $^{13}\text{C}$  spin diffusion process. Improvements are impeded by the fact that GE/Oxford/etc. does not permit investigators to modify  
54 their dDNP equipment -- for example, by adding a  $^1\text{H}$  tuning circuit to the single resonance  $^{13}\text{C}$  circuit present in their probes.  
55

56 In addition, it has been known since the 1970's that  $^1\text{H}$ 's polarize much more rapidly than low- $\gamma$  species such as  $^{13}\text{C}$  or  $^{15}\text{N}$ . For  
57 example, Hartmann, et al. (*Nuclear Instruments and Methods*, **106**, 9-12 (1973)) showed that  $^1\text{H}$ 's in alcohol samples at 1 K and 5  
58 T could be polarized in <2 minutes to levels of 35-70%.  
59

60 This paper by Elliott, et al is a description of some of the approaches to implement the  $^1\text{H} \rightarrow ^{13}\text{C}$  transfers that utilize low powers  
61 to avoid arcing in the helium atmosphere. The schemes are based on: (i) less (or low) rf-power; (ii) less overall rf-energy; (iii)  
62 simple rf-pulse shapes; and (iv) no synchronized of the  $^1\text{H}$  and  $^{13}\text{C}$  rf-irradiation. The transfer schemes are designed to take  
63 advantage of the terms in the expansion of the density matrix that go as  $I_{iz}xI_{jz}$ ; a dipolar order term that becomes important at low  
64 temperatures. The approach uses a gated microwave field and then different approaches to transfer polarization from  $^1\text{H}$  to  $^{13}\text{C}$  in  
65 Na-acetate. The paper is largely okay as written. However, I would suggest that the authors consider the following to improve the  
66 scholarship of the paper.  
67

68 The author response is given in italics.  
69

70 (Q1) I would include the reference to Hartmann (1973) above that, as far as I am aware, was the first to report the short  
71 polarization times of  $^1\text{H}$  at 1-2 K. The *d*DNP community pretty much ignores the extensive DNP physics literature from the 1960-  
72 2000 era and starts by quoting Golman and Ardenkjær-Larsen in 2003. In fact, I would suggest that they do a literature search to  
73 see if others have also reported these short polarization times.

74  
75 *(A1) A reference to Hartmann's 1973 paper has now been included.*

76  
77 (Q2) They also mention that the microwaves are gated and swept with a triangular frequency modulation. It would be good to  
78 discuss this in more detail. Why was the width of 120 MHz and a rate of 500 Hz chosen? There are AWG's available these days  
79 that can easily produce more interesting waveforms. Have any of these been introduced into the experiment? For example, the  
80 waveform could be adiabatic which might be more efficient than a simple triangular waveform.

81  
82 *(A2) The width and rate of the microwave field was optimized in order to give the best  $^1\text{H}$  polarization during active  $^1\text{H}$  DNP.*  
83 *A sentence regarding this information has been added to the manuscript: "The sample was polarized by applying microwave*  
84 *irradiation at 197.648 GHz (positive lobe of the EPR line) with triangular frequency modulation of amplitude  $\Delta f_{mw} = 120$  MHz*  
85 *(Bornet et al., 2014) and rate  $f_{mod} = 0.5$  kHz at a power of c.a. 100 mW, which were optimized prior to commencing experiments*  
86 *to achieve the best possible level of  $^1\text{H}$  polarization." Detailed information concerning microwave gating is given on page 3/line*  
87 *100 of the manuscript. More sophisticated AWG's have not been introduced into the experiment at present.*

88  
89 (Q3) Why was the TEMPO concentration set at 50 mM? This is about 3 times that used in MAS experiments and x3 the 15  
90 mM concentration of trityl often employed by Ardenkjær-Larsen and coworkers in their experiments. Does the higher concentration  
91 lead to the shorter polarization periods? A fair comparison of polarization levels and build-up times and would compare 15mM  
92 trityl to 15 mM TEMPO.

93  
94 *(A3) At present, a concentration of 50 mM of TEMPO radical is used as a "standard sample" within our laboratory, and it is*  
95 *true that the high radical concentration would lead to shorter polarization build-up times. For future experiments, in which the*  
96 *authors plan to dissolve and transfer the sample to a separate superconducting magnet for detection, we will likely use a lower*  
97 *radical concentration c.a. 25 mM TEMPO radical.*

98  
99 (Q4) Is the transfer mechanism established to be thermal mixing or the cross effect? Although this is not the focus of the paper,  
00 it should be mentioned and discussed at least briefly. If the cross effect is involved then why doesn't the *d*DNP community use  
01 nitroxide biradicals as polarizing agents. Again this could be briefly discussed.

02  
03 *(A4) For  $^1\text{H}$  nuclei at 1.2 K and 7.05 T the electron-proton transfer will presumably occur through thermal mixing and/or*  
04 *cross-effect. So far, bi-radicals have not shown better performances than TEMPO(L) in our experimental conditions. We prefer to*  
05 *keep this very complicated discussion out of the paper.*

## 06 07 **Response to Short Comment**

08  
09 This manuscript is interesting as it aims at the development of an alternative pathway (transfer via  $^1\text{H}$ ) to enhance  $^{13}\text{C}$   
10 polarization under *d*DNP conditions. The proposed  $^1\text{H}$ - $^{13}\text{C}$  transfer mechanism is different from that in the conventional Hartmann-  
11 Hahn CP, which is based on the idea of spin-locking on both the channels. The new RF scheme requires non-simultaneous RF  
12 irradiation on the two channels.

13  
14  
15  
16  
17  
18  
19  
20  
21  
22  
23  
24  
25  
26  
27  
28  
29  
30  
31  
32  
33  
34  
35  
36  
37  
38  
39  
40  
41  
42  
43  
44  
45  
46  
47  
48

Although the optimum RF power is not lower (compared to that in conventional CP), the duration of RF on  $^1\text{H}$  is significantly reduced. However that on  $^{13}\text{C}$  channel becomes significantly longer and the transfer efficiency also decreases by a factor of 2. Overall, the new approach might still be better than Hartmann-Hahn CP for technical reasons as the authors claim.

I have a few questions regarding the  $^1\text{H}$ - $^{13}\text{C}$  transfer mechanism (*the authors responses are given in italics*):

1. On page 2 line 31, the authors talk about conversion of  $^1\text{H}$  Zeeman polarization to  $I_{1z}I_{2z}$  "dipolar order" using RF. How can the proposed RF on  $^1\text{H}$  convert  $I_z$  to  $I_{1z}I_{2z}$  term, can authors provide some more insights?

*In the spin-lock frame, the magnetization shrinks to a value which is small relative to that produced by the static magnetic field (for the same sample) during the demagnetization process. This effect has been extensively covered in a number of other papers:*

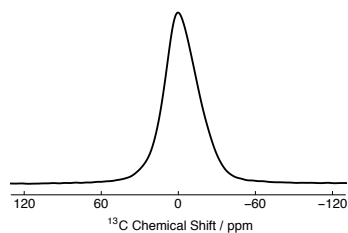
J. Jeener and P. Broekaert, *Phys. Rev.*, **1967**, 157, 232-240.  
H.-M. Vieth and C. S. Yannoni, *Chem. Phys. Lett.*, **1993**, 205, 153-156.  
J. Jeener, R. Du Bois and P. Broekaert, *Phys. Rev.*, **1965**, 139, A1959-A1961.  
A. G. Redfield, *Science*, **1969**, 164, 1015-1023.  
J.-S. Lee and A. K. Khitrin, *J. Chem. Phys.*, **2008**, 128, 114504.

*However, this is not the main focus of our current paper. Clearly, our spin system of choice is much more complicated than those in the above references (due to the presence of paramagnetic radicals etc.). Multiple dipolar orders or higher spin orders could also exist, as eluded to in our current paper. We aim to analyse these processes in greater detail in our future works.*

2. For transfer of polarization from I to S, there has to be an effective ZQ or DQ IS dipolar Hamiltonian. Since there are RF pulses on both the channels, such Hamiltonian terms can be generated. But they seem to be of higher order perturbation term in the Hamiltonian. Maybe that's the reason why transfer rate is very slow. Can authors shed some light on this?

*We surmise that since the dCP transfer is slower than conventional cross-polarization it involves a different transfer mechanism. However, we do not have sufficient insights into the true polarization transfer mechanism for this sample under dDNP conditions at present.*

3. For the given RF scheme, generating a purely ZQ or a purely DQ (IS) dipolar Hamiltonian might be challenging. This in turn may lead to phase distortion of the  $^{13}\text{C}$  signal if there are multiple  $^{13}\text{C}$  resonances. Can authors provide some  $^{13}\text{C}$  spectra?



49 *The recorded  $^{13}\text{C}$  NMR spectra do not show significant phase distortion and are detected with a good level of signal-to-noise.*  
50 *Please see the attached  $^{13}\text{C}$  NMR spectrum. Additional  $^{13}\text{C}$  NMR spectra will be provided in a following publication on a similar*  
51 *topic.*

52  
53 4. Since the method is based on  $^1\text{H}$  "dipolar order", what kind of spin-system is required for it to be efficient. Can the transfer  
54 mechanism be elucidated using a simple three-spin  $^1\text{H}$ - $^1\text{H}$ - $^{13}\text{C}$  model? How would  $^1\text{H}$  concentration in glassy matrix influence this  
55 transfer?

56  
57 *We have started simulations on a simple 3-spin-1/2  $^1\text{H}$ - $^1\text{H}$ - $^{13}\text{C}$  model system. However, agreement between simulated and*  
58 *experimental data has not yet been reached. It is this fact which provides a hint to the authors that a similar reservoir of non-*  
59 *Zeeman spin order may be used instead. There are also preliminary data to support this conclusion. Increasing the proton*  
60 *concentration of the glassy matrix dramatically decreases the polarization transfer time and increases its efficiency.*